

ESCUELA TÉCNICA SUPERIOR DE INGENIEROS
INDUSTRIALES Y DE TELECOMUNICACIÓN

UNIVERSIDAD DE CANTABRIA



Trabajo Fin de Grado

**INFLUENCE OF TEMPERATURE ON THE
CO₂/N₂ SEPARATION USING HYBRID IONIC
LIQUID-CHITOSAN MEMBRANES
(Influencia de la temperatura en la
separación de CO₂/N₂ mediante membranas
híbridas de líquido iónico-qitosano)**

Para acceder al Título de

Graduado en Ingeniería Química

Autor: Enrique Rodríguez Fernández

OUTLINE

Abstract.....	1
1. Introduction.....	2
1.1- Climate change	
1.2- Carbon Capture and Storage	
1.3- Post-Combustion capture processes: absorption vs membrane-based systems	
1.4- Solution-Diffusion mechanism in gas permeation through dense membranes	
1.5- Post combustion membrane process simulation	
1.6- Chitosan (CS)	
1.7- Ionic liquids (ILs)	
2. Objective of the project.....	11
3. Experimental Methodology.....	12
4.1- Membrane preparation	
4.2- Experimental set up: permeation plant	
4.3- Membrane characterization	
4.4- Experimental design	
4. Result Analysis.....	17
5.1- Membrane thickness, density and water uptake	
5.2- Thermal stability	
5.3- Membrane permeability	
5.4- Membrane diffusivity	
5.5- Membrane solubility	
5.6- Consistency between theoretical and empirical results	
5.7- Comparison with the state of the art: Robeson's plot	
5. Application of hybrid membranes to post combustion.....	27
6.1- Product purity vs removal efficiency	
6.2- Feed pressure required vs removal efficiency	
6.3- Membrane area required vs removal efficiency	
7. Conclusions.....	31
Nomenclature.....	33
References.....	34

ABSTRACT

Carbon capture and storage (CCS) is the technologically available method as greenhouse mitigation option, where CO₂ from fossil fuel plants is considered the main contributor. The conventional technology is chemical absorption capture, based on amines, and such solvents are energy-intensive and produce wastes due to solvent degradation. Membrane technology is considered to consume less energy and not produce waste streams. Furthermore, scale-up is facilitated by the modular design. However, the economic feasibility is limited by the transport properties of the membrane, the resistance, and the membrane material, since only polymeric membranes are commercially available yet.

In this context, new membranes are being investigated in order to improve their properties and use cheaper and more sustainable materials, avoiding dependence on petroleum-based raw materials. Hybrid membranes offer the opportunity of easily obtaining a homogeneous dispersion of two or more different materials with synergistic properties of the components. Chitosan is the second most abundant polymer from natural resources, cheap, non-toxic and biodegradable, with good film forming properties, which make it a promising sustainable material for membrane applications.

In this work, the chitosan is hybridized by the introduction of 5 wt.% ionic liquid 1-ethyl-3-methylimidazolium acetate. The permeabilities of both pure N₂ and CO₂ through chitosan and [Emim]-[Ac]-chitosan membranes have been measured at different temperatures, and adjusted to an Arrhenius-Van'Hoff model. The ionic liquid reduced the effect of temperature on membrane performance, as well as increased selectivity and the flexibility and robustness of the membrane, leading to a more suitable application to post combustion capture processes.

The permeability and selectivity values were used to estimate the performance of the new membranes in a two-stage membrane-based system to capture CO₂ from a conventional coal-fired power plant in order to evaluate the three parameters related to the technical and economic feasibility of the process: the CO₂ final purity, the feed pressure required, and the total membrane area.

1. INTRODUCTION

1.1. Climate change

Global warming has attracted increasing attention in the last century, which produced by the increase in the greenhouse gases concentration in the atmosphere, which reflect the solar radiation back to the earth surface. As a result, the temperature of our planet has increased 0.8°C during the last century (2013). This small change in the average temperature of the planet can be translated from potentially dangerous shifts in climate and weather. Carbon dioxide is mainly generated from combustion processes, which play a very important role in the energy production nowadays, so it is considered the major contributor to global warming. Because of this reason, reducing the carbon dioxide emissions is one of the most important challenges for a sustainable future.

The main actions by which these emissions are aimed at being reduced are the following ones:

- Increase the efficiency of power processes
- Use of renewable energy
- Use of nuclear energy
- Increase the energy use efficiency
- Carbon capture and storage efficiency

1.2. Carbon capture and storage

Given the early stage of development of renewable energies, the safety concerns of nuclear energy, and the high cost of hydrogen which delayed the hydrogen economy, carbon capture and storage is still the main technology to mitigate greenhouse emissions. However, the large carbon footprint of conventional capture processes makes necessary a strong effort on improving the efficiency of this technology.

CCS is a three-step process that includes:

- Capture of CO₂ from power plants or industrial processes.
- Transport of the captured and compressed CO₂ (usually in pipelines).

- Underground injection and geologic sequestration (storage) of the CO₂ into deep underground rock formations.

Only worldwide in 2012, 359 billion dollars were invested on this technology and this amount is expected to increase up to 5 trillion by 2020 (2014). In this context, Europe is the region in which the largest investment is being done, which represents the 32% of the worldwide, as represented on Figure 1.

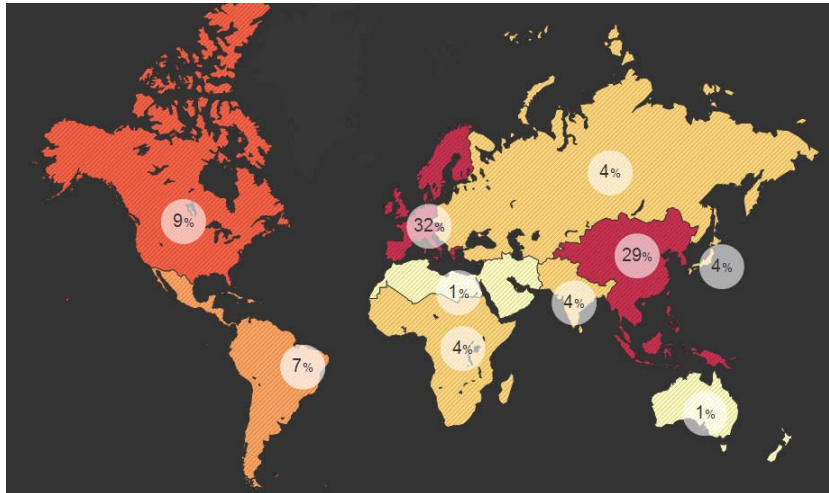


Figure 1: CCS investment nowadays worldwide (2014).

There are three strategies for CO₂ capture nowadays. Each of them employing a main gas pair separation (Merkel et al., 2010):

- Oxy-fuel combustion, which separates oxygen from air prior to combustion and produces pure CO₂ effluent.
- Post-combustion: CO₂ captured from power plant flue gas (mostly N₂ and water vapor).
- Pre-combustion: CO₂ captured from gasified coal synthesis gas (mainly H₂/CO₂ separation).

These ways are schematized on Figure 2.

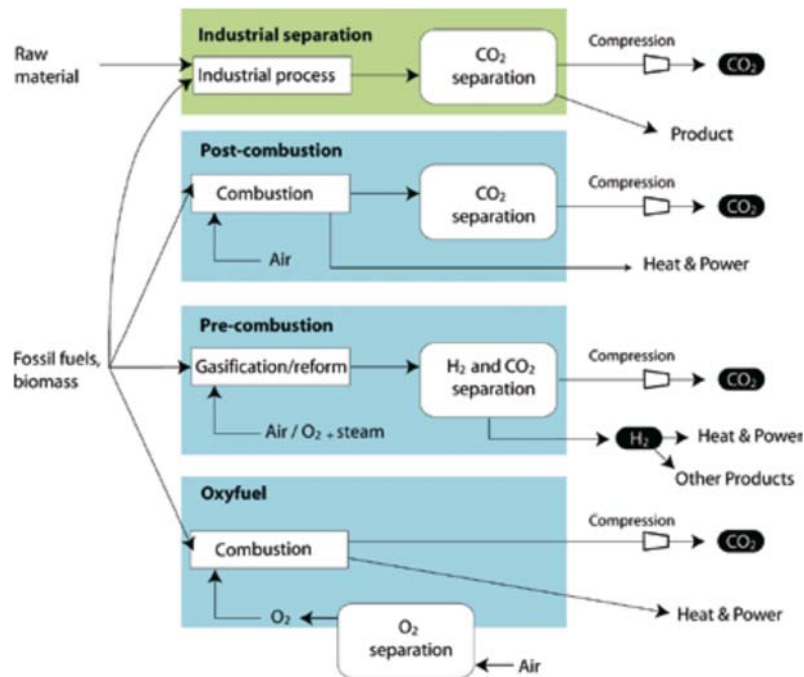


Figure 2: Carbon capture strategies (Metz et al., 2005).

1.3. Post-combustion capture processes: absorption vs membrane-based systems

The most mature technology for carbon capture from combustion processes in power plants is amine-based chemical absorption. With this technology, the cost of carbon capture is in the order of 59 €/ton CO₂ (Zhai and Rubin, 2013)

This process is composed of two main stages:

- Absorption of carbon dioxide in the solvent, mainly amine-based compounds with high affinity of acid gases, at low temperatures and high pressures, which benefit the solution process.
- Desorption and solvent regeneration in the stripping stage at high temperatures and low pressures in order to recover the carbon dioxide.

The performance of this technology is shown in the Figure 3.

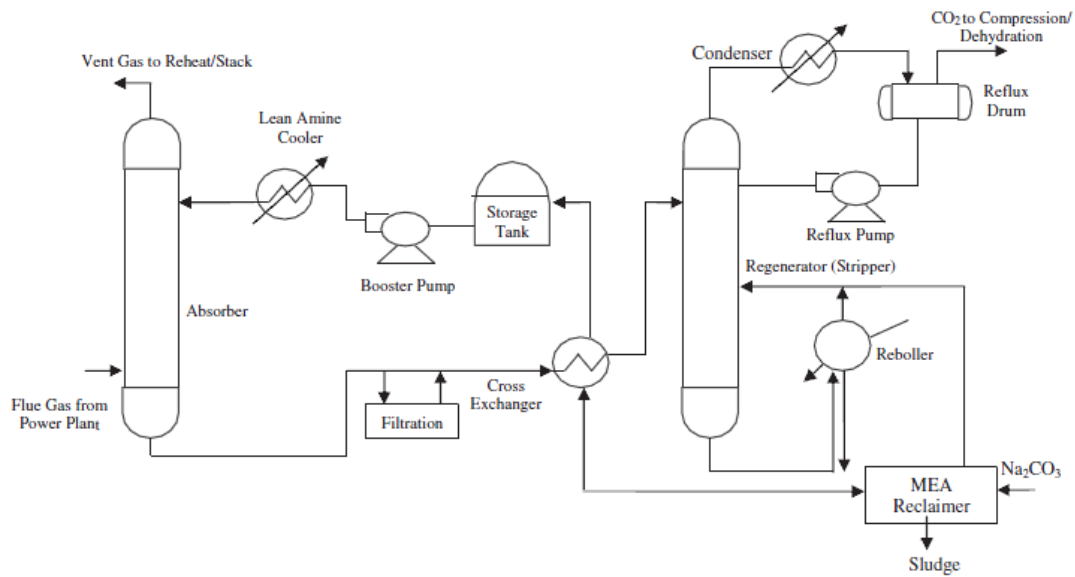


Figure 3: Process flow diagram of a typical chemical absorption system for CO₂ recovery from flue gas (Olajire, 2010)

However, the use of this technology has several drawbacks:

- The process consumes considerable energy.
- Solvent degradation and equipment corrosion occur in the presence of O₂.
- SO_x and NO_x in the gas stream react with solvents and form non-regenerating, heat-stable salts that must be purified.

Because of these reasons, membrane technology has become a promising alternative for capture processes. The main advantages of membrane technology are the following:

- No regeneration energy is required.
- Simple modular system.
- No waste streams are produced.

Nevertheless, membranes have also several drawbacks which must be faced:

- Membranes can be plugged by impurities.
- Membrane stability in the presence of water vapor.
- The technology has not been proven industrially yet, although some pilot plants studies have been reported.
- Thermal stability limits at operation conditions.
- Membrane fabrication and cost.

Nevertheless, membrane technology is expected to achieve carbon capture prices in the range of 40-60 \$/ton CO₂, depending on the membrane transport properties and the material price (Zhai and Rubin, 2013).

The properties of a membrane to be competitive with conventional absorption-based capture processes are thus:

- High carbon dioxide permeability.
- High CO₂/N₂ selectivity.
- High thermal and mechanical resistance.
- Stable performance in the presence of water vapor.
- Low cost and easy to manufacture.

Currently, the available commercial membranes are made of polymers such as silicon rubber, cellulose acetate or Polydimethylsiloxane (Ramasubramanian et al., 2013):

- Polaris (MTR,USA)
- Pervap4060 (Sulzer, Germany)
- Separex (France)

The commercial membranes are still suffering from low mechanical, thermal and chemical stability, and inability to work in the presence of water vapor, challenges which limit the study of their long-term and large-scale operation.

1.4. Solution-Diffusion mechanism in gas permeation through dense membranes

The gas permeation through dense polymeric membranes is usually described by the solution-diffusion mechanism (Cussler, 1997):

- a) Adsorption of the gas onto the membrane material
- b) Diffusion across the membrane
- c) Desorption in the permeate side

Both the adsorption and desorption steps can be described by the Henry's law:

$$C_i = S \cdot p_i \quad (7)$$

where C_i is the gas concentration in the membrane surface, p_i is the gas partial pressure and S is a proportional parameter that describes the solubility of the gas in the membrane material, and exhibits van't Hoff temperature dependence:

$$S_i = S_{i,0} \cdot e^{-\frac{\Delta H_{S,i}}{R \cdot T}} \quad (8)$$

where ΔH_s is the heat of sorption, kJ/mole, R the ideal gas constant, T the temperature in Kelvin and S_0 the front factor derived from the van't Hoff plot.

The diffusion step is described by the Fick's law:

$$J_i = -D_i \frac{dC_i}{dx} \quad (9)$$

where J_i is the flux of the gas through the membrane ($\text{mol} \cdot \text{m}^{-2} \cdot \text{s}^{-1}$), C_i is the gas concentration ($\text{mol} \cdot \text{m}^{-3}$), and D_i is the diffusivity coefficient of the gas i in the membrane material ($\text{m}^2 \cdot \text{s}^{-1}$), which exhibits the same temperature dependence as the Henry's constant due to its thermal character:

$$D_i = D_{i,0} \cdot e^{-\frac{E_{D,i}}{R \cdot T}} \quad (10)$$

where $E_{D,i}$ is the activation energy for diffusion of gas i .

Combining equations (7) and (9), the following expression is derived to describe the transport of a component through a dense membrane:

$$J_i = -D_i \cdot S_i \frac{dp_i}{dx} \quad (11)$$

Applying a mass balance to the membrane material, the following equation is obtained:

$$J_i = -D_i \cdot S_i \frac{(p_{i,f} - p_{i,p})}{\delta} = -P_i \frac{(p_{i,f} - p_{i,p})}{\delta} \quad (12)$$

where P_i is the permeability coefficient, δ is the membrane thickness, $p_{i,f}$ is the partial pressure of the gas i in the feed side and $p_{i,p}$ is the partial pressure of the gas i in the permeate side.

As a result, it is seen that the permeability is the product of diffusivity (kinetic factor) and solubility (thermodynamic factor), known as the solution-diffusion model:

$$P = D \cdot S \quad (13)$$

1.5. Post combustion membrane process simulation

The use of membranes in industrial post-combustion processes to separate and purify the carbon dioxide can be estimated from the permeability and selectivity values of the membrane materials and have an idea of the membrane area and pressure conditions needed to carry out a carbon capture process, following the study developed by Zhai and Rubin (2013), who developed a statistical model based on their studies of post-combustion carbon capture membrane processes in a power plant of 550 net electrical output MW.

This capture process is depicted in Figure 5:

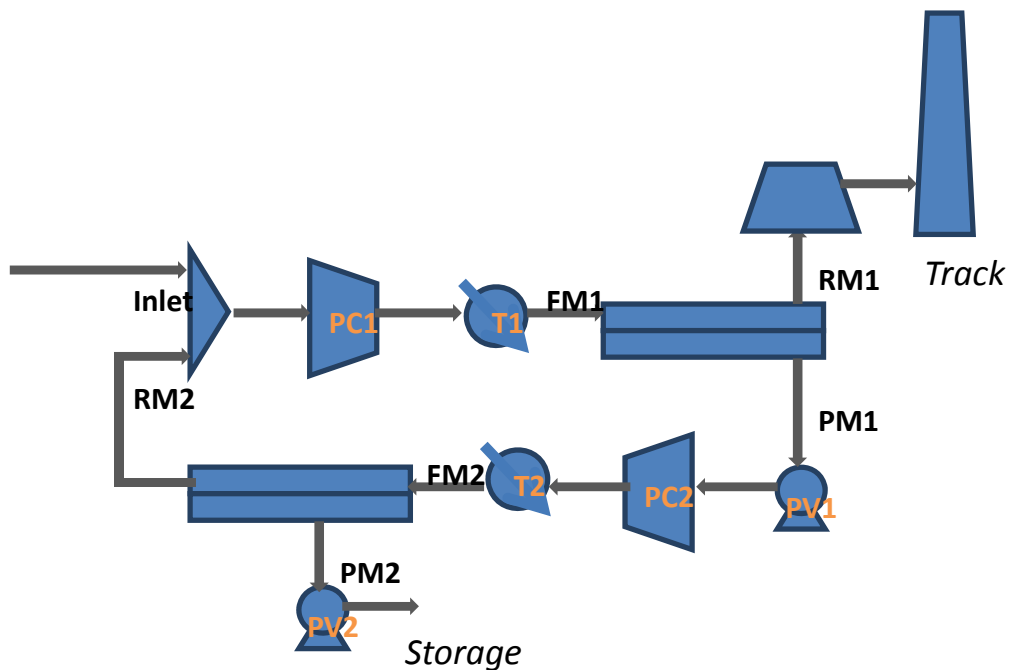


Figure 5: Process flow sheet diagram. RM: membrane retentate; PC: feed pressure; PV: vacuum pressure.

The main variables involved in this process are the temperature, the composition of each stream, specially the inlet and the two output streams, the membrane area of each stage and the pressure conditions achieved by both compressors and vacuum pumps. The use of vacuum pumps is justified thus decreasing the total cost of the process, creating a pressure ratio between the feed and permeate side of the membrane by not only compressing the inlet stream, but also applying vacuum to the permeate,

which has a lower molar flow rate value, and, as a result, a lower energy demand (Merkel et al., 2010).

Following the methodology developed by Zhai and Rubin (2013), some parameters of this process can be evaluated as function of input parameters related to the membrane transport properties and some process specifications, as it is described in this section.

Model input parameters:

- CO₂ removal efficiency: fraction of the total inlet CO₂ which leaves the system as CO₂ product at high purity to storage or valorize (η): a range of 50-90% has been considered.
- CO₂ concentration of inlet flue gas (x): 15% has been considered.
- Ideal membrane selectivity (α).
- Membrane CO₂permeance (GPU) (τ).
- Permeate side pressure (P_p): 0.1 bar has been considered.

Model output parameters:

- CO₂ purity achieved (y).
- Pressure ratio through the membrane and feed pressure (ϕ):

$$\phi = \frac{\text{Feed side pressure}}{\text{Permeate side pressure}} \quad (1)$$

- Total membrane area required (A).

Model equations:

Pressure ratio:

$$\text{Ln}(\phi) = 10.5 - 36.6 \cdot x + 93.6 \cdot x^2 - 6.73 \cdot \eta + 5.63 \cdot \eta^2 - 0.0889 \cdot \alpha + 0.00059 \cdot \alpha^2 \quad (2)$$

CO₂ product purity:

$$y = 0.589 + 1.51x - 0.0337 \cdot \eta - 0.00164 \cdot \alpha + 0.0131 \cdot \text{Ln}(\phi) - 0.794 \cdot S_1 \quad (3)$$

Total membrane area:

$$\frac{\ln(A \cdot \tau)}{2} =$$

$$23.8 + 7.17x + 15.7y + 4.4 \cdot \eta + 0.077\alpha - 2.32 \cdot \ln(\phi) - 00167 \cdot S_1 - 11.9 \cdot S_2 \quad (4)$$

Stage cut 1 and 2 (intermediate parameters):

$$S_1 = -0.249 + 1.29 \cdot x + 0.336 \cdot \eta + 0.000732 \cdot \alpha - 0.0123 \cdot \ln(\phi) \quad (5)$$

$$S_2 = 0.9 - 0.207 \cdot \eta - 0.00295 \cdot \alpha - 0.331 \cdot S_1 \quad (6)$$

1.6. Chitosan (CS)

Moreover, the commercially available polymer membranes are produced from petroleum-derived chemicals and since still a large membrane area is required for membrane technology to be competitive with conventional absorption processes, this adds to the necessity of developing novel membrane materials with better performance.

Environmental awareness and stricter regulations on wastes have directed focus to use of biopolymers from renewable resources instead of synthetic polymers. Chitosan is one of those, poly[$\beta(1-4)$ -2-amino-2-deoxy-D-glucopyrenose], a linear polysaccharide obtained by the dehydration of chitin, an abundant natural polymer (Figure 4).

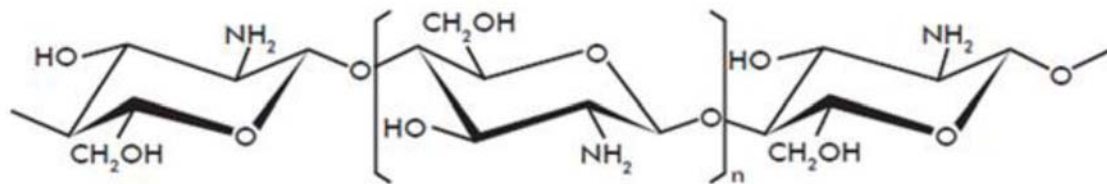


Figure 4: Chitosan chemical structure (Krajewska, 2005).

The main properties of chitosan for its application as CO₂ selective membrane material are:

- Good film forming properties.
- Ion exchange capacity, leading to good interaction with either other membrane components or gas molecules.

- Hydrophilicity, which makes it stronger in wet conditions and improve its transport properties, making it a suitable material to work in post-combustion conditions.
- Basic character due to the amino and hydroxyl groups, which provides selectivity towards carbon dioxide.

The main drawbacks are swelling capacity and low mechanical strength.

1.7. Ionic liquids (ILs)

Ionic liquids are organic liquid salts with melting points below 100°C, constituted by organic cations and organic or inorganic anions, whose chain size provide conformational flexibility.

Other interesting properties are:

- Thermal stability at high temperatures.
- Non-flammability.
- Negligible vapor pressure, and as such they have been proposed to replace amines in capture from flue gases.
- Great variety of anion-cation combinations (10^8), which make them “design solvents”. RTILs that contain the acetate anion exhibit strong affinity towards CO_2 .

In this work, 1-ethyl-3-methylimidazolium acetate ([Emim][Ac], IL) ionic liquid has been selected because of its high CO_2 selectivity in CO_2/N_2 separation as SILM (Santos et al., 2014). The chitosan is expected to have good interaction properties with this ionic liquid (Xie et al., 2006), thus implying that a small amount of IL would improve the selectivity and robustness of the membranes towards carbon dioxide.

2. OBJECTIVE OF THE PROJECT

- Synthesis of new hybrid membranes, which take advantage of both the mechanical and thermal strength, biodegradability and low cost of Chitosan and the CO_2 selectivity (in terms of solubility difference) of the ionic liquid 1-ethyl-3-methylimidazolium acetate.

- Characterization and measurement of their transport properties, solubility, diffusivity and permeability, at different temperatures, in order to study their temperature-dependence performance.
- Study of the behavior of these membranes in a 2 stage membrane-based system to capture CO₂ from a conventional coal-fired power plant, taking into account the temperature and membrane material influence in the efficiency in terms of membrane area (related to capital cost), pressure required (related to operating cost) and product purity (related to storage cost).

3. EXPERIMENTAL METHODOLOGY

3.1. Membrane preparation

a) Pure chitosan (CS) membranes

Chitosan is dissolved in diluted acetic acid aqueous solution. For preparing 100 g 2wt.% polymer solution, the following quantities are used:

- 2 g chitosan (Aldrich, coarse ground flakes and powder)
- 4 g glacial acetic acid (Panreac, purity>99%)
- 94 g distilled water

The mixture is heated at 80°C and stirred for 24 hours under reflux. Then, the viscous polymer solution is vacuum filtered to remove remaining impurities. The membranes were prepared then by casting 10 mL on a polystyrene Petri dish, and the solvent was evaporated at room temperature for several days. Once the membrane is dried, it can be removed from the Petri dish and the thickness is measured using a Mitutoyo digital micrometer (IP65, Japan) with 0.01 mm precision. Before permeation experiments, the membrane is immersed in a NaOH solution 1 mol/L for one hour, to exchange the acetate functional groups and free the hydroxyl and amino groups that provide basic character and CO₂ affinity to the membrane material. The membranes were carefully washed several times with distilled water to remove the excess NaOH and stored at 4°C to keep the properties constant before permeation measurements.

b) Ionic Liquid-Chitosan (IL-CS) hybrid membranes

A similar procedure is followed to prepare ionic liquid-chitosan hybrid membranes. The hybrid solution was prepared by mixing 7.6 g chitosan solution are mixed with 0.4 g of 1-ethyl-3-methylimidazolium acetate Ionic Liquid (Aldrich, assay $\geq 96,5\%$, $C_8H_{14}N_2O_2$ CAS No. 143314-17-4), in order to obtain solution proportion IL:CS of 5wt.%. This mixture is stirred during 24 hours, and casted on a Petri dish to dry for one week. After measuring thickness and density, the membranes were also treated in NaOH 1 mol/L and rinsed with distilled water and kept at 4°C before permeation.

3.2. Experimental set up: permeation plant

The permeability of the membranes is measured in discontinuous mode, using the constant volume setup depicted in Figure 6, where the membrane module is submerged in a water bath in order to control temperature.

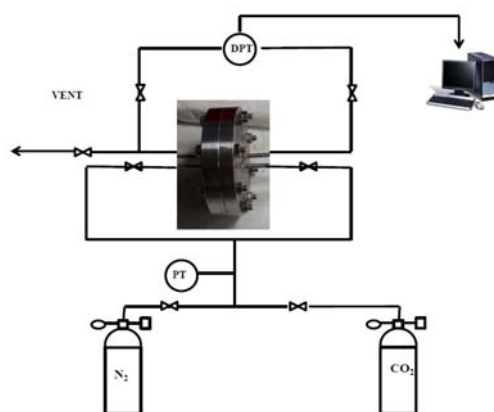


Figure 6: experimental setup diagram.

The membrane module is connected, by means of pneumatic valves, to the feed and permeate sides. A single and a differential transducer (Omega, UK) measure the pressure level in the feed side and the pressure difference across the membrane during the whole experiment, in order to monitor the gas volume that goes through it. The permeation cell is composed by two parts pneumatically pressed each other on a Viton ring that seals the membrane. The membrane is placed over a stainless steel permeation cell leading to an effective area of 14.05 cm².

The main steps in these experiments are:

- Filling of feed and permeate sides of the membrane module up to a pressure of 2-3bar.
- Closing the valves to the compartments, and open the vent valve to make the driving force across the membrane.
- Monitoring the differential pressure between both compartments as a function of time, in order to determine the transport properties of the membrane:

3.3. Membrane characterization

Membranes are characterized in order to determine the following properties:

- Thickness: it influences the value of the permeability coefficient according to equation (12). It has been measured with a Mitutoyo micrometer (IP 65, Japan).
- Density: it is calculated from the gravimetrically measured weight of the membrane and it provides information on the processability of the gas molecules in the membrane matrix. Besides, it can be used to determine the amount of reactants needed to fabricate the membranes and the calculations of solubility coefficients (equation 17).

The densities of the dry membranes have been measured relating both the mass and the geometric properties of the membrane:

$$\text{Density}\left(\frac{\text{g}}{\text{cm}^3}\right) = \frac{\text{mass (g)}}{\text{thickness (cm)} \cdot \frac{\pi}{4} \cdot \text{diameter(cm)}^2} \quad (15)$$

- Water uptake: The water uptake is the parameter that quantifies the water adsorbed by the membrane material. It is also a measure of the swelling capacity and hydrophilicity.

$$\text{Water Uptake (\%)} = \frac{\text{mass}_{\text{after humidification}} - \text{mass}_{\text{before humidification}}}{\text{mass}_{\text{before humidification}}} \cdot 100 \quad (16)$$

It is very important to control this parameter as much as possible, due to the effect of water (as a carrier) in the CO₂ transport, affecting the results obtained and their reproducibility.

- Mechanical resistance has been measured in a Zwick/Roell Universal Testing machine by the following parameters:
 - Tensile strength (MPa): it provides an idea of the maximum pressure that the membrane is capable to stand without breaking.
 - Elongation at break (%): it provides an idea of the flexibility of the membrane material.
- Thermal resistance: Thermo gravimetric analyses (TGA) were performed in a DTG 60H Shimadzu instrument (Japan) in air from 25 to 700 °C at a heating rate of 10 °C/min, in order to study the thermal stability of the resulting membranes.
- Solubility: The CO₂ and N₂ sorption of the membrane material was measured in a TA –DTG 60H Shimadzu thermo balance, at a constant temperature in the range 25- 55°C using 2-3 mg sample. The solubility is then calculated using the density of the membrane material and given in cm³(STP)/cm³-cmHg in the solution diffusion model (equation (13)).

$$S \left(\frac{\text{cm}^3 \text{STP}}{\text{cm}^3 \cdot \text{cm Hg}} \right) = \frac{\text{Gas adsorbed (mg)} \cdot \text{Membrane density} \left(\frac{\text{mg}}{\text{cm}^3} \right) \cdot 0.0224 \frac{\text{cm}^3 \text{STP}}{\text{mol}}}{\text{Membrane (mg)} \cdot \text{Pressure (cm Hg)} \cdot \text{Gas mol weight} \left(\frac{\text{mg}}{\text{mol}} \right)} \quad (17)$$

- Permeability and diffusivity: These are also intrinsic parameters of the transport through the membrane materials (equation (13)) and can be measured by single –gas permeation experiments in a constant volume setup described in the next paragraph.
- Membrane ideal selectivity: This parameter defines the separation ability of a certain membrane material and is calculated as the ratio between pure gas permeabilities of CO₂ and N₂.

$$\alpha_{\text{CO}_2/\text{N}_2} = \frac{P_{\text{CO}_2}}{P_{\text{N}_2}} \quad (18)$$

The permeability is measured analyzing the evolution of the pressure difference with time. Applying a mass balance to both cameras when the steady state is reached, the following expression is obtained (Cussler, 1997):

$$\text{Ln} \left(\frac{\Delta p_0}{\Delta p} \right) = (\beta \cdot P / \delta) \cdot t \quad (19)$$

Where Δp is the pressure difference between permeate and feed side, P is the permeability coefficient of the penetrating gas, δ is the membrane thickness and β is a geometric factor dependent on the gas permeation set-up (Figure 6):

$$\beta = A \cdot \left(\frac{1}{V_{\text{feed}}} + \frac{1}{V_{\text{permeate}}} \right) = 1110 \text{ m}^{-1} \quad (20)$$

The diffusivity is measured by the “time lag” method (Bara et al., 2007). The time lag is calculated from the representation of total volume accumulated in the permeate side vs time, as seen in Figure 7.

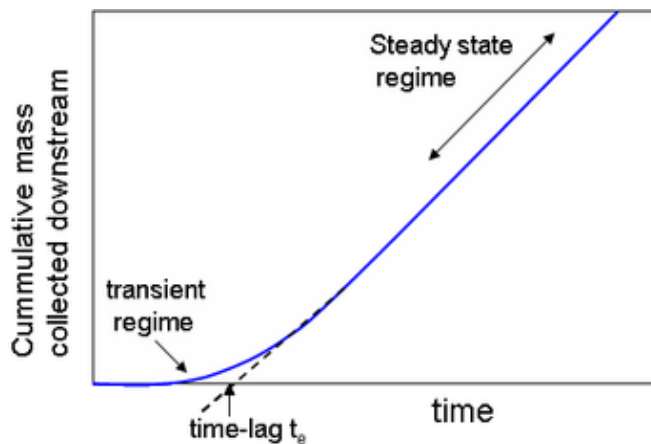


Figure 7: Time-lag calculation from experimental data.

Thus, the diffusivity can be estimated with the following expression:

$$D = \frac{\delta^2}{6 \cdot t_e} \quad (21)$$

3.4. Experimental design

Several experiments have been carried out in order to determine the transport properties of the membranes as a function of temperature. These experiments have covered the following variables:

- Membrane material: Chitosan (CS) and Ionic Liquid-Chitosan (IL-CS).
- Gas measured: N_2 and CO_2 (in this order).
- Temperature: 25°C, 30°C, 40°C and 50°C.

Furthermore, more than one experiment has been carried out in order to ensure the reproducibility of the results.

4. RESULT ANALYSIS

4.1. Membrane thickness, density and water uptake

The membrane parameters providing information on the morphology or structure of the membrane material that have measured are: thickness, density, water uptake, as collected in the following table.

Table 1: Membrane characterization results.

	Thickness (μm)	Density (g/cm^3)	Water Uptake (%)
CS	125 ± 39	0.74 ± 0.12	271 ± 46
IL + CS	350 ± 133	1.17 ± 0.39	3.96 ± 1.93

The addition of the ionic liquid increases the membrane density, and reduces drastically the water uptake capacity. The increased density may be related to the reduced void volume accounting for a good interaction between the ionic liquid and the chitosan. The decrease in water uptake is especially significant taking into account the fact that the water contain affects the transport properties of the membrane, so in general, the highest the water uptake, the lowest the reproducibility of the transport properties measurements.

Table 2 shows the tensile strength and elongation at break of CS and IL-CS hybrid membrane materials, agreeing with literature on CS membranes.

Table 2: Mechanical strength properties of both CS and IL-CS membrane material (Casado-Coterillo et al. 2014).

	Tensile strength (MPa)	Elongation at break (%)
CS	31.63 ± 7.41	18.52 ± 8.23
IL (5%) – CS	16.09 ± 11.04	40.44 ± 12.45
CS (Xu et al., 2011)	59.1 ± 5.3	15.5 ± 3.0

4.2. Thermal stability

Figure 8 represents the thermo gravimetical analyses of the IL, CS and IL-CS hybrid membranes.

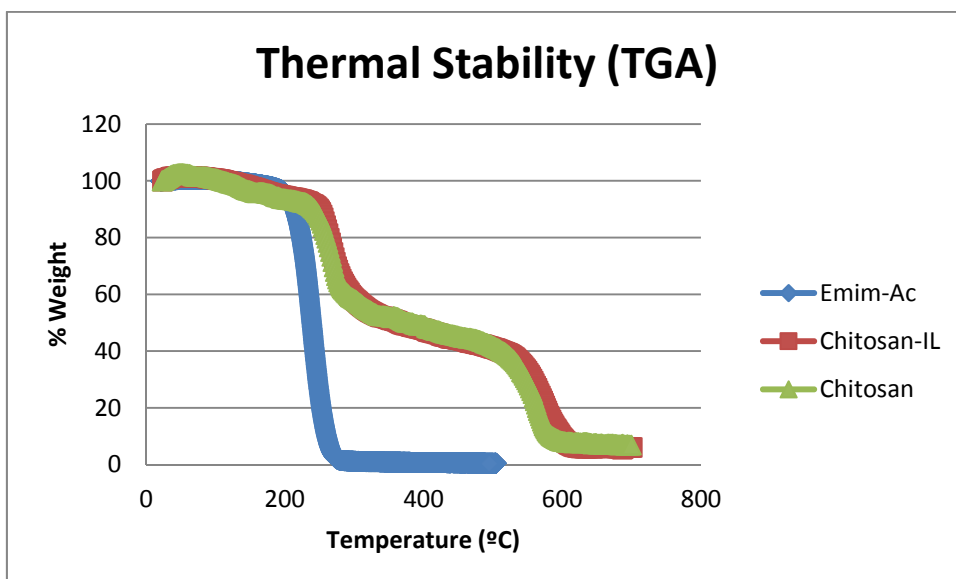


Figure 8: Thermal resistance of membrane materials.

The decomposition temperature was calculated as the temperature at which 5% wt. loss occurs (Table 3). Two thermal decomposition stages are seen in the TGA analysis corresponding to a first dehydration stage, and then, the decomposition of the material, as characteristic of chitosan. The addition of the ionic liquid improves slightly the thermal resistance of the membrane material.

Table 3: Thermal decomposition of the different materials

Material	Thermal decomposition temperature (°C)
IL	203.4
CS	184.4
IL-CS	191.9

These data give an idea of the maximum temperature at which these membranes are allowed to work in the process. Because of the typical temperature of the industrial

post-combustion processes, which is usually lower than 100°C, these membranes exhibit enough thermal resistance for the purpose for which they are intended.

4.3. Membrane permeability

The permeabilities of both N₂ and CO₂ have been measured and adjusted to an Arrhenius relationship (equation 8) in order to evaluate the temperature influence of the different types of membrane.

- Pure Chitosan Membranes (CS)

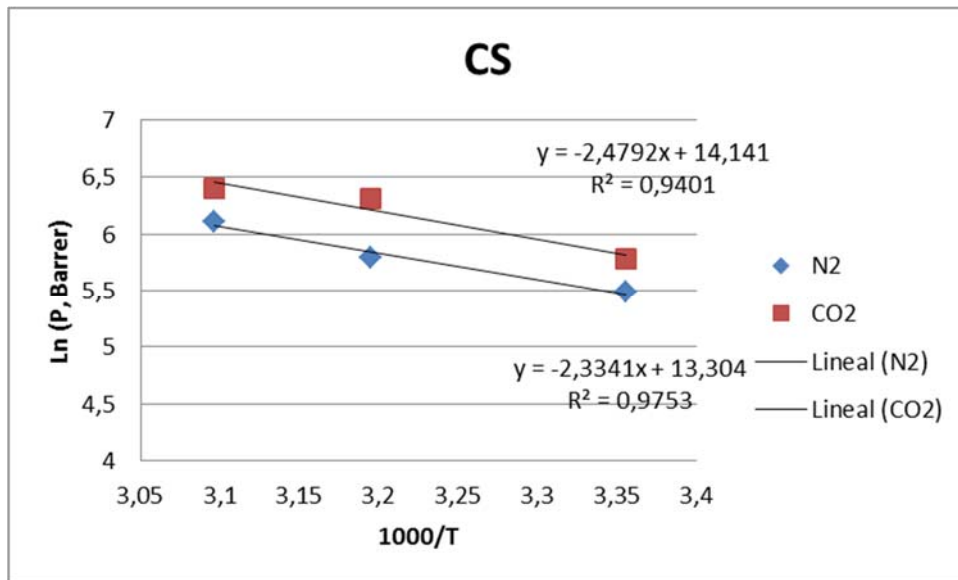


Figure 9: Permeability of N₂ and CO₂ as a function of temperature in Arrhenius form for pure CS membranes.

The permeability of both N₂ and CO₂ increases with temperature in pure polymer membranes with very similar activation energies, because the ideal selectivity ratio is as low as 1.45.

Table 4: Activation energies for permeation and front factors of N₂ and CO₂ permeabilities in chitosan membranes.

	Nitrogen	Carbon Dioxide
P_0 (Barrer)	$1.38 \cdot 10^6$	$5.97 \cdot 10^5$
E_p (kJ/mol)	20.8	19.4

- Ionic liquid - Chitosan membranes

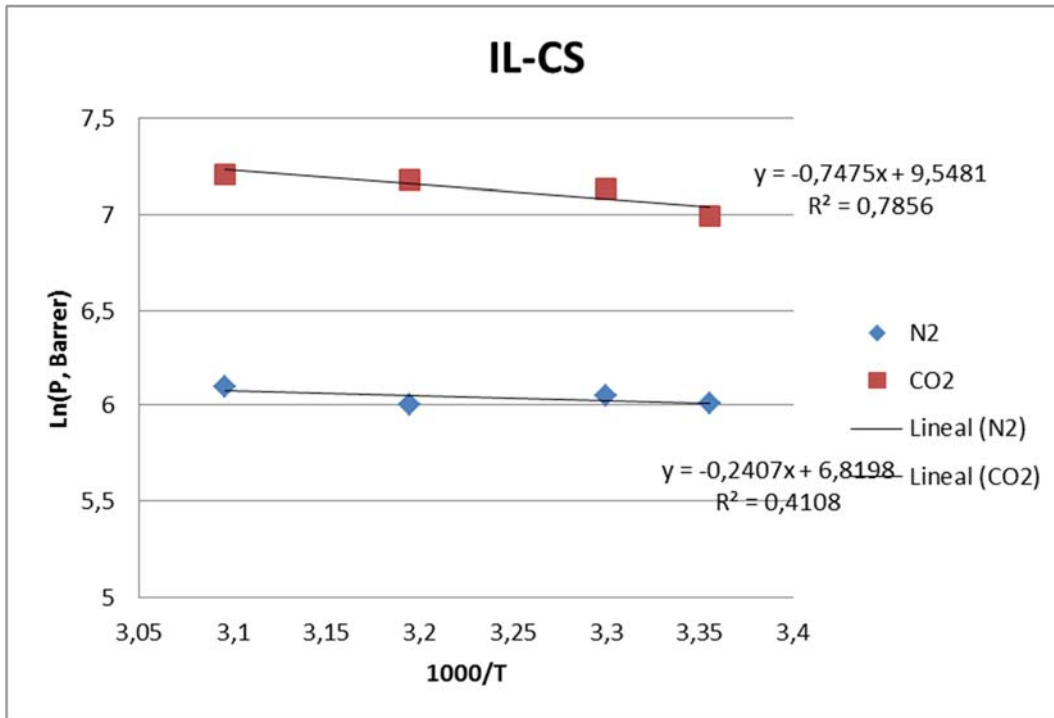


Figure 10: Permeability of N₂ and CO₂ as a function of temperature in Arrhenius form in IL-CS membranes.

Table 5: Activation energies for permeation and front factors of N₂ and CO₂ permeabilities in IL-CS membranes.

	Nitrogen	Carbon Dioxide
P_0 (Barrer)	$9.15 \cdot 10^2$	$1.4 \cdot 10^4$
E_p (kJ/mol)	2.0	6.2

The addition of IL in the membrane increases CO₂ permeability around 2.5 times, as it was expected due to the high solubility of carbon dioxide in [Emim][Ac]. Furthermore, the activation energies for permeation of both gases are significantly reduced, since a reduction of the temperature influence on the transport properties was observed upon

IL addition. This allows expecting a easier adaptation to different thermal operating conditions.

4.4. Membrane diffusivities

The diffusivities dependence with temperature follows also an Arrhenius-behavior with temperature, as is depicted in Figures 11 and 12.

- Pure Chitosan Membranes (CS)

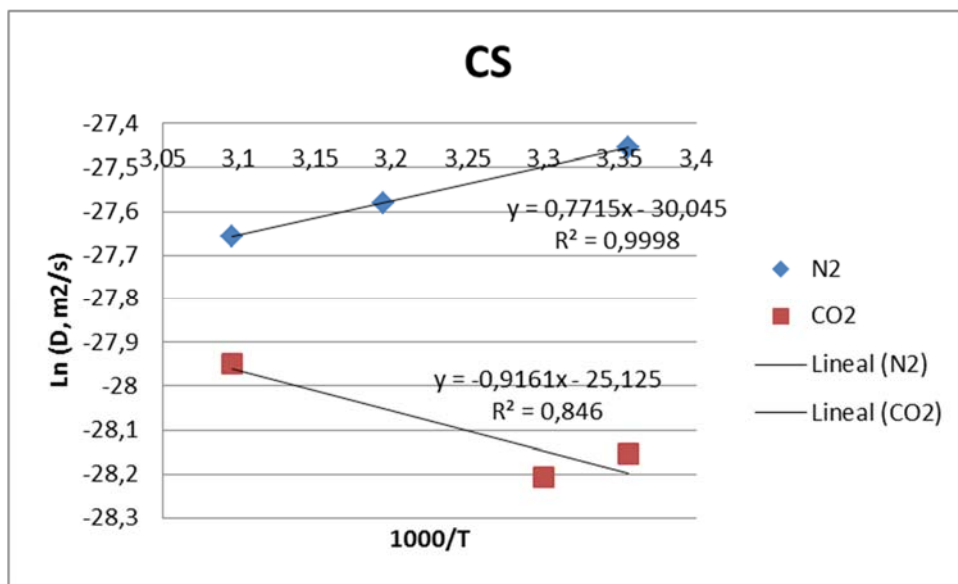


Figure 11: Diffusivities of N₂ and CO₂ as a function of temperature in Arrhenius form in CS membranes.

Table 6: Activation energies for diffusion and front factors of N₂ and CO₂ diffusivities in CS membranes.

	Nitrogen	Carbon Dioxide
D ₀ (m ² ·s ⁻¹)	9.00·10 ⁻¹⁴	1.23·10 ⁻¹¹
E _D (kJ/mol)	-6.4	7.6

- IL-CS Membranes

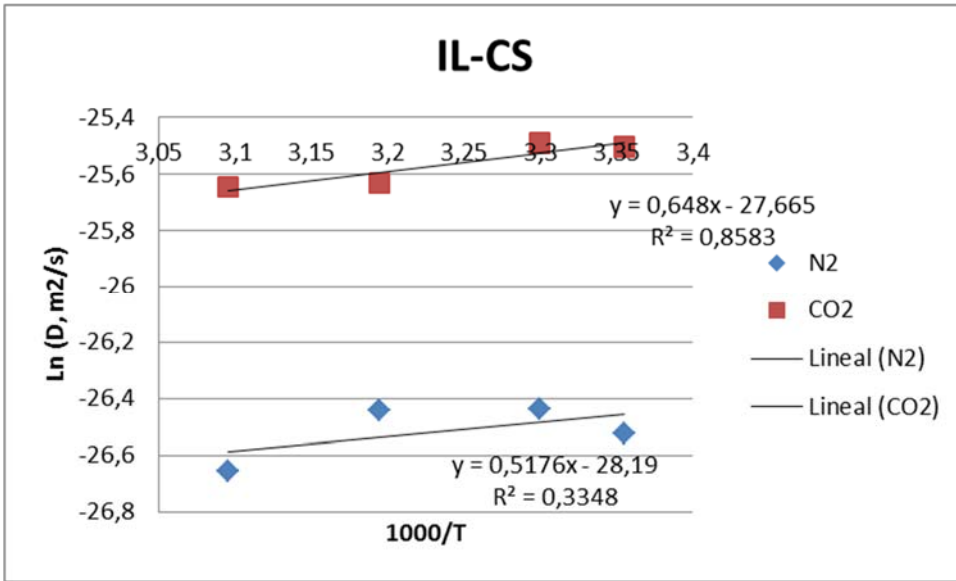


Figure 12: Diffusivity of N₂ and CO₂, respectively, as function of temperature in Arrhenius form in IL-CS membranes.

Table 7: Activation energies for diffusion and front factors of N₂ and CO₂ diffusivities in IL-CS membranes.

	Nitrogen	Carbon Dioxide
D_0 (m ² ·s ⁻¹)	$5.72 \cdot 10^{-13}$	$9.71 \cdot 10^{-13}$
E_D (kJ/mol)	-4.3	-5.4

4.5. Membrane solubilities

The solubilities dependence with temperature follows a van's Hoff relationship, according to equation (17), as depicted in Figures 13 and 14.

- CS Membranes

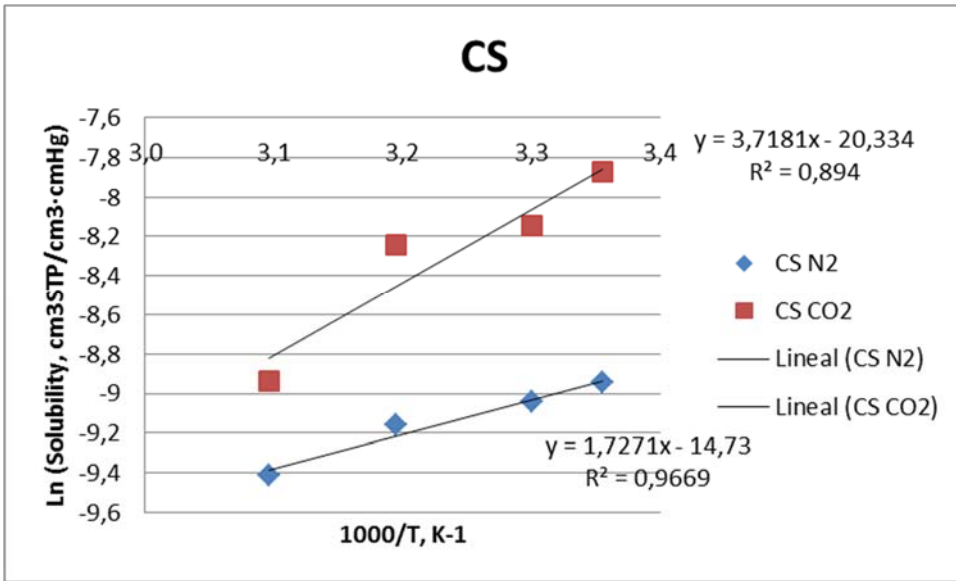


Figure 13: Solubility of N₂ and CO₂, respectively, as a function of temperature in van't Hoff equation form for CS membranes.

Table 8: Heat of sorption and solubility front factors of N₂ and CO₂ solubilities in CS membranes.

	Nitrogen	Carbon Dioxide
S ₀ (cm ³ STP·cm ⁻³ ·cm Hg ⁻¹)	4.01·10 ⁻⁷	1.48·10 ⁻⁹
ΔH _s (kJ/mole)	14.4	30.9

The heat of sorption agrees with literature values (El-Azzami et al., 2007), and it is decreased for N₂ thus employing a higher separation ability in the hybrid IL-CS membranes.

- IL-CS Membranes

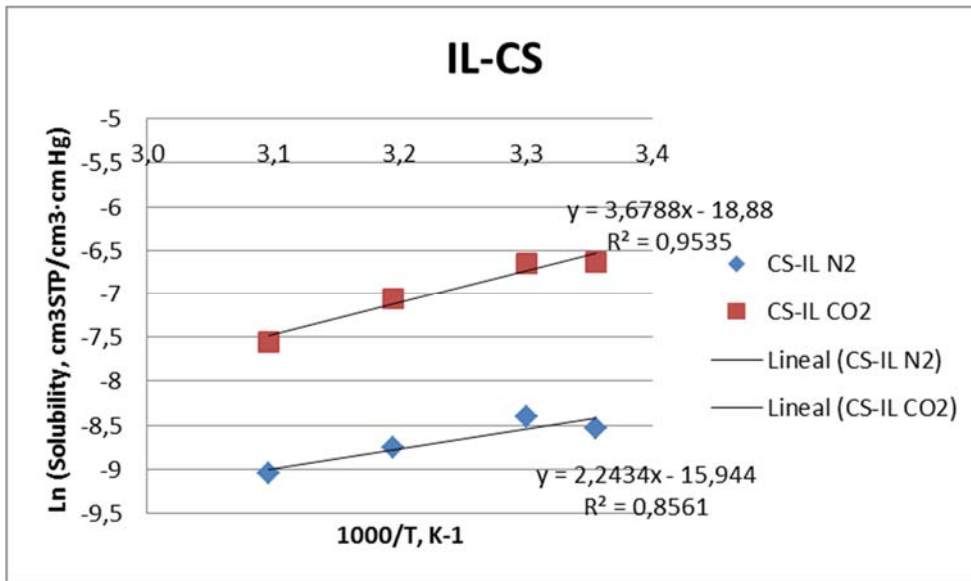


Figure 14: Solubility of N₂ and CO₂ as a function of temperature in Arrhenius form in IL-CS membranes.

Table 9: Heat of sorption and solubility front factors of N₂ and CO₂ solubilities in IL-CS membranes.

	Nitrogen	Carbon Dioxide
S ₀ (cm ³ STP·cm ⁻³ ·cm Hg ⁻¹)	1.19·10 ⁻⁷	6.32·10 ⁻⁹
ΔH _s (kJ/mol)	18.6	30.6

4.6. Consistency between theoretical and empirical results

Permeability, diffusivity and solubility of both N₂ and CO₂ have been experimentally measured in this work for both CS and hybrid IL-CS membranes. These parameters in polymeric membranes usually respond to the solution-diffusion model described in equation (20), which established the relationship:

$$P(\text{barrer}) = 10^{-10} \cdot D(\text{cm}^2 \cdot \text{s}^{-1}) \cdot S(\text{cm}^3\text{STP} \cdot \text{cm}^{-3} \cdot \text{cm Hg}^{-1}) \quad (20)$$

In this work, there is a discrepancy between the diffusivity values obtained from the time-lag equation (12), “Experimental” in Tables 10 and 11, and those calculated

using the ratio of experimental permeability and solubility according to solution – diffusion model in equation (20), “Theoretical” in Tables 10 and 11.

The following results have been obtained:

- Pure Chitosan membranes (CS):

Table 10: Comparison of N₂ and CO₂ diffusivities (cm²·s⁻¹) in CS membranes (both empirical and theoretical).

T (°C)	Nitrogen		Carbon Dioxide	
	Experimental	Theoretical	Experimental	Theoretical
25	1.19·10 ⁻⁰⁸	6.37·10 ⁻⁰⁵	5.93·10 ⁻⁰⁹	2.50·10 ⁻⁰⁴
30	6.33·10 ⁻⁰⁹	1.73·10 ⁻⁰⁴	5.62·10 ⁻⁰⁹	1.97·10 ⁻⁰⁴
40	1.05·10 ⁻⁰⁸	1.24·10 ⁻⁰⁴	1.27·10 ⁻⁰⁸	5.25·10 ⁻⁰⁴
50	9,76·10 ⁻⁰⁹	3,43·10 ⁻⁰⁴	7.28·10 ⁻⁰⁹	7.43·10 ⁻⁰⁴

- Ionic liquid + Chitosan (IL-CS):

Table 11: Comparison of N₂ and CO₂ diffusivities (cm²·s⁻¹) in IL-CS membranes (both empirical and theoretical).

T (°C)	Nitrogen		Carbon Dioxide	
	Experimental	Theoretical	Experimental	Theoretical
25	3.03·10 ⁻⁰⁸	3.10·10 ⁻⁰⁵	8.39·10 ⁻⁰⁸	5.51·10 ⁻⁰⁴
30	3.30·10 ⁻⁰⁸	3.25·10 ⁻⁰⁵	8.49·10 ⁻⁰⁸	5.60·10 ⁻⁰⁴
40	3.29·10 ⁻⁰⁸	4.73·10 ⁻⁰⁵	7.40·10 ⁻⁰⁸	8.33·10 ⁻⁰⁴
50	2.65·10 ⁻⁰⁸	8.46·10 ⁻⁰⁵	7.29·10 ⁻⁰⁸	1.14·10 ⁻⁰³

These results exhibit a difference between the experimental diffusivity and the theoretical calculated by the solution-diffusion model. These differences can be considered an evidence of a more complex transport mechanism through these hybrid membranes than that observed in dense polymer membranes, which cannot be described by this solution-diffusion transport mechanism.

4.7. Comparison with the state of the art of membrane materials: Robeson's plot

In 1991, Robeson published a review of the permeabilities and ideal selectivities for different polymeric materials for the most applied pair gas separations in order to compare the separation capacities of different materials. A trade-off between permeability and selectivity was observed: the higher the permeability, the lower the permeability for most of the polymer materials represented. This compromise between both properties was described by equation (21),

$$P = k \cdot \alpha^n \quad (21)$$

Where k and n are empirical parameters.

In 2008, these correlations were revised for updated polymer membranes and newly developed membrane materials, and the correlation in equation (21) updated each gas separation processes. The case of the CO₂/N₂ separation was first included, by equation (22) left as follows:

$$P_{CO_2} = 3.0967 \cdot 10^7 \cdot \alpha_{CO_2/N_2}^{-2.8888} \quad (22)$$

The results obtained for the membranes developed in this work are compared with the so-called "Robeson" upper bound, which has since become a benchmark for comparison of newly developed membrane materials with existing ones, as it can be observed in Figure 15.

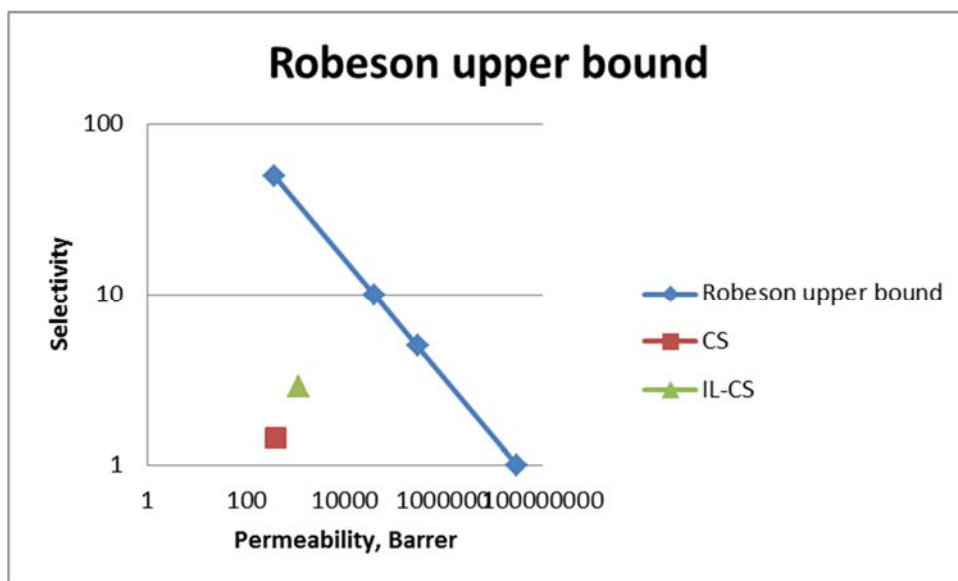


Figure 15: Robeson upper bound for CO₂/N₂.

As seen in figure 15, although the permselectivity of the hybrid membranes prepared in this work is still below the upper bound. The addition of ionic liquid in the polymer matrix increases both the permeability and the selectivity of the CS membrane.

5. APPLICATION OF HYBRID MEMBRANES TO POST COMBUSTION

The permeability and selectivity values obtained experimentally for the novel membranes prepared in this work have been applied to study the potential use in industrial post-combustion processes on the separation and purification of carbon dioxide from flue gas mixtures, mainly N_2 . In particular, the membrane area and pressure conditions were calculated in order to obtain a determined CO_2 purity at the exit in a power plant as explained above, following the statistical model developed by Zhai and Rubin (2013).

5.1. Product purity vs removal efficiency

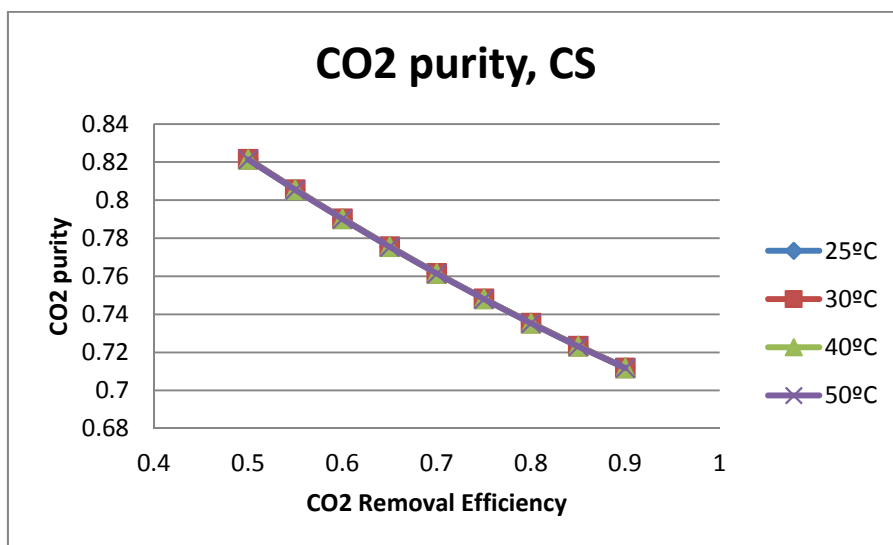


Figure 16: Temperature effect on CO_2 final purity using CS membranes.

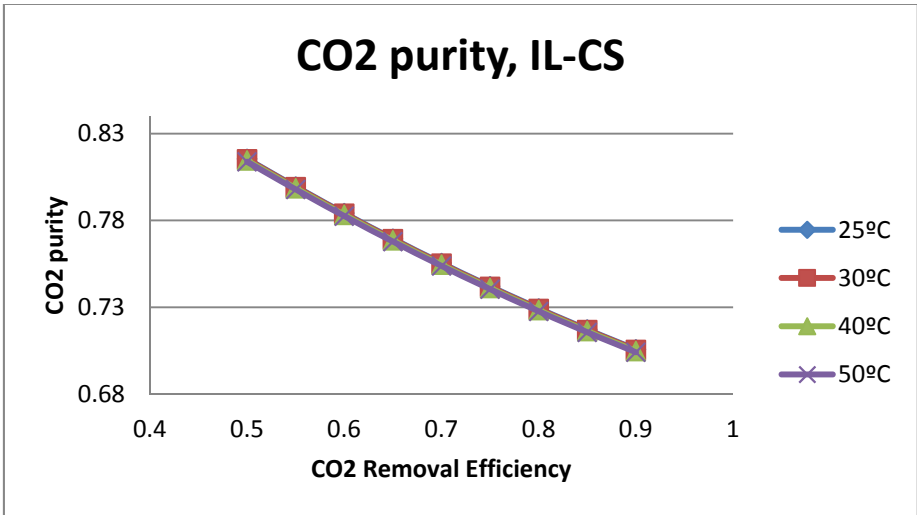


Figure 17: Temperature effect on CO₂ final purity using IL-CS membranes.

The purity that can be estimated to achieve with these CS and IL-CS membranes is in the range 60-80% from the inlet CO₂ composition of 15%, with for removal efficiencies of 50-90%. This purity decreases as the removal efficiency increases, showing that there is a compromise between both factors. Moreover, these results are almost independent not only on temperature, but also on the membrane composition, showing that the sensitivity of this parameter to the membrane properties for both CS and IL-CS membranes is low. The main effect of purity in the final cost of the processes would be related with the storage cost.

5.2. Feed pressure required vs removal efficiency

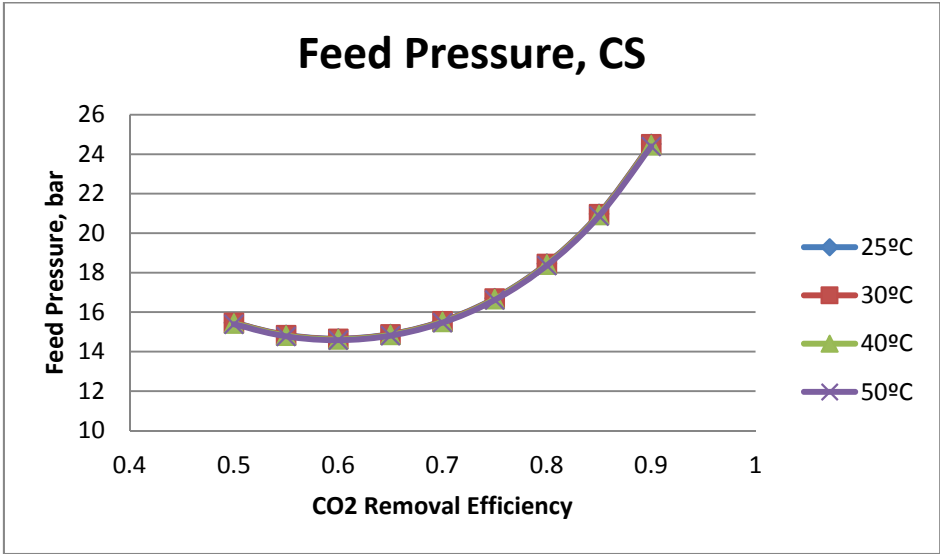


Figure 18: Temperature influence on feed pressure required using CS membranes.

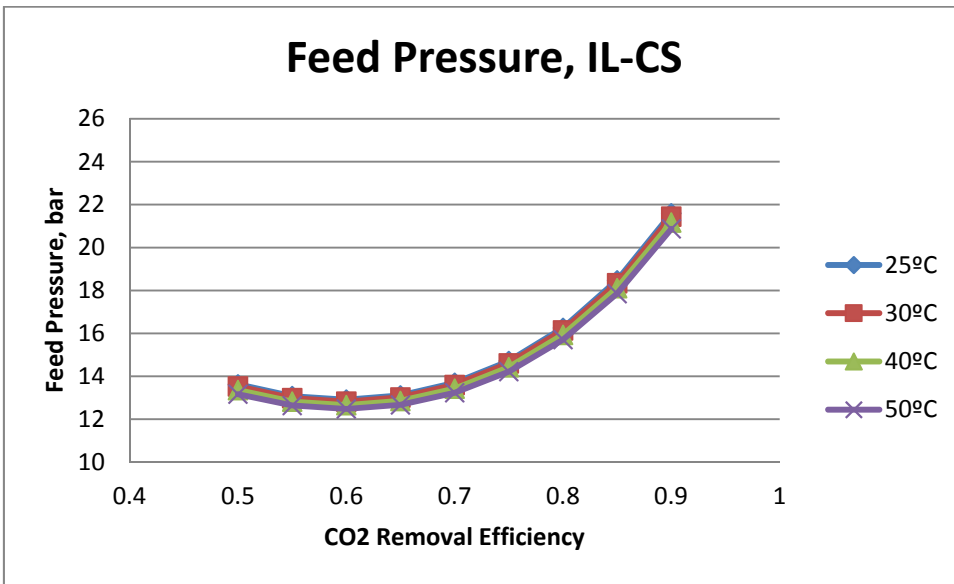


Figure 19: Temperature influence on feed pressure required using IL-CS membranes.

The required feed pressure does not follow a constant behavior as function of removal efficiency. The minimum value of feed pressure required leads to a removal efficiency of 60%. The temperature influence is very low, and there is a significant difference between the behavior of CS and IL-CS membrane, which requires a lower feed pressure, and is expected to decrease the operating cost of the capture process.

5.3. Membrane area required vs removal efficiency

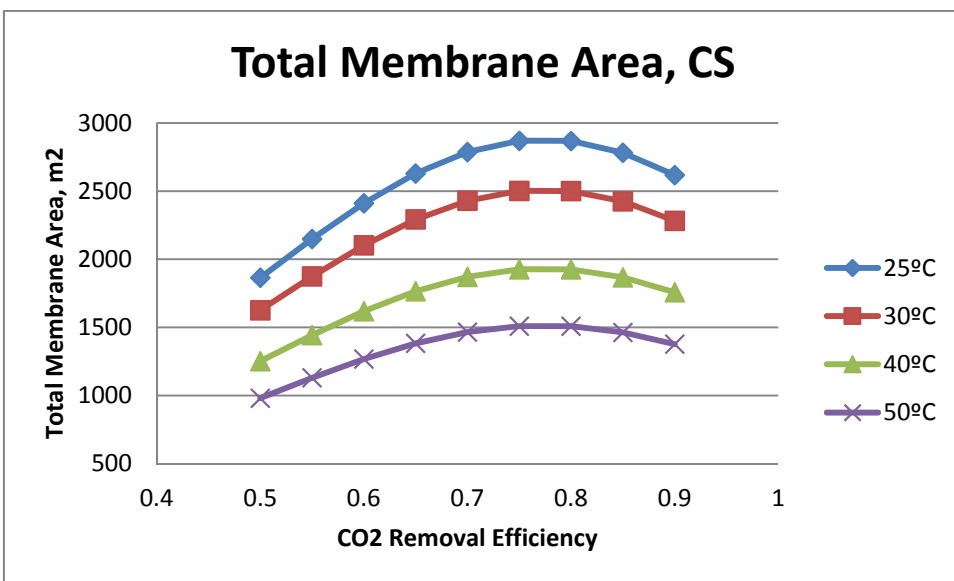


Figure 20: Temperature influence on total membrane area required using CS membranes.

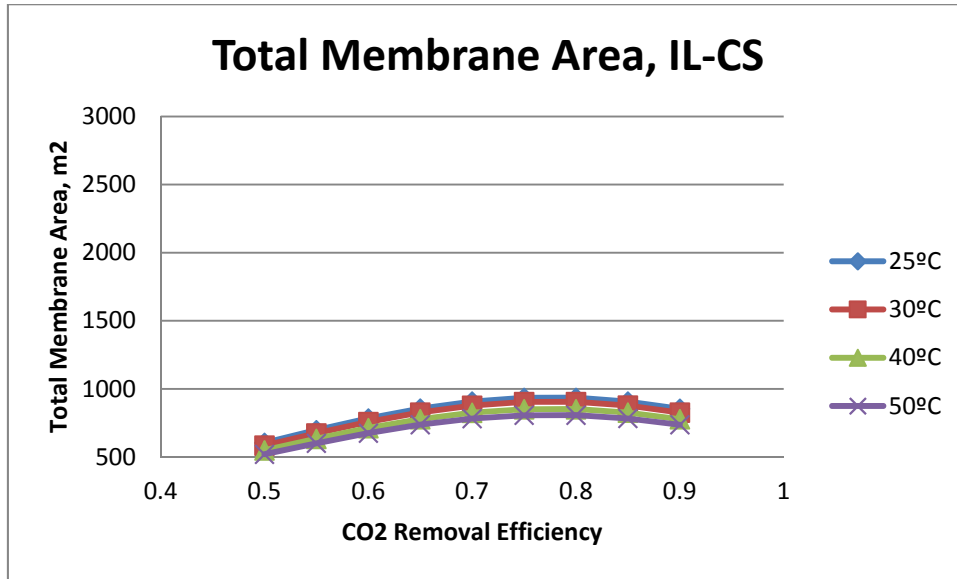


Figure 21: Temperature influence on total membrane area required using CS-IL membranes.

The required membrane area for a certain removal efficiency is represented in Figures 20 and 21 for CS and hybrid IL-CS membranes. It provides information on the material requirements, which in a further study, would be related to the capital cost of the capture process.

This is the major difference observed for the new hybrid IL-CS membrane materials developed in this work. This membrane area is observed to decrease with temperature in pure CS membranes, while almost constant in IL-CS membranes. These facts can be explained by the relation between the membrane area and the CO₂ permeability, which are inversely proportional. The enhancement in the CO₂ permeability in IL-CS membranes leads to a lower membrane area, and the lower activation energy of the CO₂ permeability leads to a lower sensitivity with temperature.

6. CONCLUSIONS

Hybrid IL-CS membranes have been prepared and characterized in terms of their thermal and mechanical strength, showing an enhancement with respect to pure CS membranes. The mechanical strength of IL-CS membranes is lower than that of CS membranes, but the flexibility is greatly improved, thus the membranes are robust enough to withstand the feed pressure and temperature required by the industrial application.

The influence of temperature on solubility, diffusivity and permeability has been described using Arrhenius-van't Hoff equations and activation energies calculated there from.

The addition of a small amount of IL in the CS membrane matrix increases the CO₂ solubility, thus increasing the permeability and selectivity with respect to the pure polymer. The activation energy for CO₂ permeation is higher than that of N₂, which is related to the enhanced selectivity and permeability of the IL-CS membranes with respect to pure CS membranes.

The addition of IL reduces the temperature dependence of the permeability and diffusivity, thus reducing the values of the activation energies, which gives scope to believe the membranes to adapt at different working temperatures.

The solution-diffusion model does not describe the transport properties of hybrid IL-CS membranes as that of pure polymer membranes, thus a more complex mechanism should be derived in order to provide an accurate prediction of permeation through dense novel membranes.

The addition of the IL reduces the water uptake capacity of the pure CS membranes, which is expected to modify the CO₂/N₂ performance and facilitate the reproducibility of the membrane synthesis and performance.

The permeability and selectivity values of CS and IL-CS membranes were introduced in a two-stage membrane capture process system simulation, achieving a CO₂ purity in the range of 70-80%, which decreases with removal efficiencies from 90 to 50%.

The improvement on the permeability and selectivity values on hybrid IL-CS membranes leads to a lower pressure and membrane area required for the capture process, thus reducing both the operating and the investment cost of the process.

Further research is being conducted on the development of hybrid membranes based on polymerizable ILs and acetate-based ionic polymers with large CO₂ solubility and never used in membrane technology so far.

NOMENCLATURE

D diffusion coefficient ($\text{m}^2 \text{s}^{-1}$)

D_0 front factor of diffusion ($\text{m}^2 \text{s}^{-1}$)

E_D activation energy of diffusion (kJ mol^{-1})

E_p activation energy of permeation (kJ mol^{-1})

ΔH_s heat of sorption (kJ mol^{-1})

P gas permeability (Barrer)

P_0 front factor of gas permeability (Barrer)

P_f pressure in the feed compartment (Pa)

P_p pressure in the permeate compartment (Pa)

Δp pressure difference between feed and permeate compartments (Pa)

R ideal gas constant ($\text{bar L mol}^{-1} \text{K}^{-1}$)

S gas solubility coefficient ($\text{cm}^3(\text{STP}) \cdot \text{cm}^{-3} \cdot \text{cm Hg}^{-1}$)

S_0 front factor of gas solubility coefficient ($\text{cm}^3(\text{STP}) \cdot \text{cm}^{-3} \cdot \text{cm Hg}^{-1}$)

T temperature (K)

t time (s)

θ time lag (s)

β geometric factor of the membrane permeation setup (m^{-1})

δ membrane thickness (m)

x: CO_2 molar fraction of post-combustion stream

y: molar purity of CO_2 product

α : ideal membrane selectivity

φ : membrane pressure ratio

η : CO_2 removal efficiency (%)

τ : membrane CO_2 permeance (GPU)

A: total membrane area

S_1 : stage cut in stage 1

S_2 : stage cut in stage 2

REFERENCES

Bara, J. E., Gabriel, C. J., Lessmann, S., Carlisle, T., Gin, D. L., & Noble, R. D. (2007). Polymerized room temperature ionic liquids as gas separation membranes. *Industrial and Engineering Chemistry Research*, 46, (16), 5397-5404.

Casado-Coterillo, C., López-Guerrero, M. M., Irabien, A. (2014) Synthesis and characterisation of ETS-10/Acetate-based ionic liquid/chitosan mixed matrix membranes for CO₂/N₂ separation. *Membranes*, 4, (2), 287-301.

Cussler E.L. (1997) Diffusion. Mass Transfer in Fluid Systems, 3rd ed., Cambridge University Press: Cambridge, UK. 655pp.

El-Azzami, L. A. and Grulke, E. A. (2007). Dual mode model for mixed gas permeation of CO₂, H₂, and N₂ through a dry chitosan membrane. *Journal of Polymer Science, Part B: Polymer Physics*, 45(18), 2620-2631.

He, X., and Hägg, M.-B. (2012). Membranes for environmentally friendly energy processes. *Membranes*, 2(4), 706-726.

Huang, Y., Merkel, T. C., & Baker, R. W. (2014). Pressure ratio and its impact on membrane gas separation processes. *Journal of Membrane Science*, 463, 33-40.

Krajewska, B. (2005). Membrane-based processes performed with use of chitin/chitosan materials. *Separation and Purification Technology*, 41(3), 305-312.

Low, B. T., Zhao, L., Merkel, T. C., Weber, M., Stolten, D. (2013). A parametric study of the impact of membrane materials and process operating conditions on carbon capture from humidified flue gas. *Journal of Membrane Science*, 431, 139-155.

Metz, B., Davidson, O., Coninck, H. de, Loos, M., Meyer, L. (2005) IPCC Special Report on Carbon Dioxide Capture and Storage. Intergovernmental Panel on Climate Change, Cambridge University Press: Cambridge, New York, USA. 442pp.

Merkel, T. C., Lin, H., Wei, X., & Baker, R. (2010). Power plant post-combustion carbon dioxide capture: An opportunity for membranes. *Journal of Membrane Science*, 359(1-2), 126-139.

Olajire, A. A. (2010). CO₂ capture and separation technologies for end-of-pipe applications - A review. *Energy*, 35(6), 2610-2628.

Ramasubramanian, K., Zhao, Y. and Winston W.S. Ho (2013). CO₂ capture and H₂purification: Prospects for CO₂-selective membrane processes. *AIChE Journal*, 59, 1033-1045.

Robeson, L. M. (2008). The upper bound revisited. *Journal of Membrane Science*, 320(1-2), 390-400

Santos, E., Albo, J., & Irabien, A. (2014). Acetate based supported ionic liquid membranes (SILMs) for CO₂ separation: Influence of the temperature. *Journal of Membrane Science*, 452, 277-283.

The Global Landscape of Climate Finance Report (2013) [Online, last consulted on 30-06-2014]: <http://www.climatefinancelandscape.org/>

US Environmental Protection Agency [Online, last consulted on 30-06-2014]: <http://www.epa.gov/>

Xie, H., Zhang, S., & Li, S. (2006). Chitin and chitosan dissolved in ionic liquids as reversible sorbents of CO₂. *Green Chemistry*, 8(7), 630-633.

Xu D., Loo L. S., Wang K. Characterization and diffusion behavior of chitosan-POSS composite membranes. *Journal of Applied Polymer Science*, 122,427-435.

Zhai, H. and Rubin, E. S. (2013).Techno-economic assessment of polymer membrane systems for postcombustion carbon capture at coal-fired power plants. *Environmental Science and Technology*, 47(6), 3006-3014.

Zornoza, B., Gorgojo, P., Casado, C., Téllez, C., & Coronas, J. (2011).Mixed matrix membranes for gas separation with special nanoporous fillers. *Desalination and Water Treatment*, 27(1-3), 42-47.